



Published in final edited form as:

Nat Commun. ; 3: 869. doi:10.1038/ncomms1874.

O-glycosylation modulates integrin and FGF signaling by influencing the secretion of basement membrane components

E Tian¹, Matthew P. Hoffman², and Kelly G. Ten Hagen^{1,*}

¹Developmental Glycobiology Unit, Laboratory of Cell and Developmental Biology, National Institute of Dental and Craniofacial Research, National Institutes of Health, Bethesda, MD 20892-4370, USA

²Matrix and Morphogenesis Section, Laboratory of Cell and Developmental Biology, National Institute of Dental and Craniofacial Research, National Institutes of Health, Bethesda, MD 20892-4370, USA

Abstract

Extracellular microenvironments play crucial roles in modulating cell interactions during development. Here we discover that a conserved protein modification (O-glycosylation) influences extracellular matrix (ECM) composition during mammalian organogenesis, affecting integrin signaling and FGF-mediated cell proliferation. Specifically, mice deficient for an enzyme (*Galnt1*) that adds sugars to proteins during early stages of organogenesis resulted in intracellular accumulation of major basement membrane (BM) proteins and ER stress, with resultant effects on FGF signaling, epithelial cell proliferation and organ growth. Exogenous addition of BM components rescued FGF signaling and the growth defects in a $\beta 1$ -integrin-dependent manner. Our work demonstrates for the first time that O-glycosylation influences the composition of the ECM during mammalian organ development, influencing specific aspects of the ER stress response, cell signaling, cell proliferation and organ growth. Our work provides insight into the role of this conserved protein modification in both development and disease.

Keywords

basement membrane; extracellular matrix; FGF signaling; integrin; ER stress; O-glycosylation; protein glycosylation; microenvironment; submandibular gland; development

Introduction

The cellular microenvironment is a vast array of components that surround cells and tissues, modulating basic processes such as cell adhesion, differentiation, proliferation and signaling. The crucial importance of this extracellular matrix (ECM) is illustrated in diseases where changes in the constitution of the matrix are accompanied by altered cell proliferation and morphology associated with tumor progression and metastasis¹⁻⁴. While many factors are known to influence the composition of the cellular environment, the inherent complexities

*Address correspondence to: Kelly G. Ten Hagen, Ph.D., Building 30, Room 426, 30 Convent Drive, MSC 4370, Bethesda, MD 20892-4370. Tel: 301-451-6318; Fax: 301-402-0897; Kelly.Tenhagen@nih.gov.

Author Contributions

E.T. and K.G.T.H. designed and planned the research with input from M.P.H.; E.T. performed the experiments; E.T., M.P.H. and K.G.T.H. analyzed and discussed the data; K.G.T.H. wrote the paper with input from E.T. and M.P.H.

Competing financial interests: The authors declare no competing financial interests.

associated with the synthesis, processing, transport and secretion of the diverse components indicate many levels of regulation that are yet to be discovered.

The basement membrane (BM) is a specialized ECM microenvironment surrounding all epithelia during mammalian development. BMs form structural scaffolds for tissue morphogenesis, and also regulate cell proliferation and signaling events during development by serving as ligands for receptors as well as reservoirs for growth factors and other bioactive molecules^{5,6}. The two major BM components present in developing mammalian organs are collagen and laminin. While collagen mediates BM stability in many developing tissues, laminin is required for BM formation, as mice deficient in laminin $\alpha 1$, $\beta 1$ or $\gamma 1$ lack BMs and die during early embryogenesis^{5,6}.

Murine embryonic submandibular gland (SMG) development and growth are regulated by components of the BM⁷⁻¹². Intact collagen IV present within the BM provides structural integrity⁵, while the proteolytic NC1 fragments serve to regulate epithelial proliferation and end bud expansion via PI3K-AKT signaling¹¹. Likewise, laminin within the BM serves as both a scaffold for cell-matrix interactions as well as a ligand that mediates fibroblast growth factor (FGF) signaling through $\beta 1$ integrin receptors^{6,12}. Roles for the ECM proteins perlecan and fibronectin in gland clefting and growth have also been demonstrated^{7,10}. Components of the BM are also rich in sugar-based modifications, including heparan sulfate glycosaminoglycans (GAGs) and O-linked glycans^{10,13,14}. Specific GAG structures modulate FGF signaling by influencing receptor-ligand interactions^{10,14}. However, the roles for additional sugars present within the BM are unknown.

Recent work highlights the critical regulatory roles of sugar-based protein modifications in many aspects of development and disease¹⁵⁻²¹. The two major types of sugar linkages present on secreted proteins are N-linked (to asparagine) and O-linked GalNAc (to serine or threonine). N-linked glycosylation regulates protein folding, secretion and stability; disruption of N-glycosylation activates all branches of the ER stress response and induces cellular apoptosis^{22,23}. Roles for O-linked glycosylation have been more difficult to decipher given the functional redundancy present amongst the 20 enzymes (ppGalNAcTs) responsible for initiation of this type of glycosylation in mammals^{16,24}. While studies in model organisms have demonstrated that certain members of this family are essential for viability²⁵⁻²⁸, the redundancy present in mammals has hampered our understanding of the specific functions of these enzymes in human health and development. Nonetheless, alterations in protein O-glycosylation are associated with an increased risk of certain forms of cancer in humans and are also responsible for two other diseases, familial tumoral calcinosis and Tn syndrome²⁹⁻³³. Additionally, genome-wide association studies have identified genes encoding O-glycosyltransferases among those associated with triglyceride and high density lipoprotein (HDL) cholesterol levels, thus implicating protein O-glycosylation in cardiovascular disease risk³⁴⁻³⁶. While these studies highlight the impact of this evolutionarily conserved modification in human health, the mechanistic basis for the specific role of O-glycosylation in mammalian development and disease is largely unknown.

Here we investigate the function of protein O-glycosylation during mammalian organogenesis by examining mice deficient for the O-glycosyltransferase ppGalNAcT-1³⁷. Loss of the gene encoding ppGalNAcT-1 (*Galnt1*) reduces cell proliferation and SMG growth by specifically disrupting the secretion of BM components, resulting in decreased integrin and FGF signaling. Additionally, we provide evidence that loss of O-glycosylation induces a subset of ER stress responses that are distinct from those induced upon the loss of N-linked glycosylation. We propose that *Galnt1*-dependent O-glycosylation specifically regulates the composition of the cellular microenvironment during development by influencing BM protein secretion. This work provides a mechanism by which the loss of O-

glycosylation may contribute to disease susceptibility by influencing ECM composition and the proteostasis network.

Results

Loss of *Galnt1* affects SMG growth during early development

We used qPCR to determine which of the 19 murine *Galnt* gene family members were expressed during SMG development (Supplementary Fig. S1a). *Galnt1* was found to be the most abundantly expressed family member in embryonic day 12 (E12) SMGs (Supplementary Fig. S1b), suggesting a potential role for *Galnt1* during early stages of SMG development. SMG development begins at E11.5 and then at E12, the SMG is visible as an initial, single epithelial end bud on a duct, surrounded by condensing mesenchyme (Fig. 1b). As development proceeds, the end bud enlarges via epithelial cell proliferation and undergoes cleft formation to begin the process of branching morphogenesis. Successive rounds of proliferation and clefting, as well as duct specification and elongation, result in an arborized glandular structure at later stages of development.

Galnt1-deficient mice have been described previously as being viable but having lymphocyte homing defects and bleeding disorders of unknown etiology³⁷. We examined the effects of *Galnt1* loss on SMG growth and development by crossing *Galnt1*^{+/-} heterozygotes and analyzing SMGs from wild type (*Galnt1*^{+/+}), heterozygous (*Galnt1*^{+/-}) and *Galnt1*-deficient (*Galnt1*^{-/-}) E12 littermates. qPCR analysis of SMGs demonstrated a specific loss of *Galnt1* and no compensatory up or down regulation of other members of the family in *Galnt1*-deficient SMGs (Fig. 1a). E12 SMG buds from *Galnt1*^{-/-} animals were significantly smaller than both wild type and heterozygous littermates, as determined by measurement of the end bud perimeter and diameter (Fig. 1b, c). Additionally, E14 SMGs from *Galnt1*^{-/-} animals were significantly smaller than littermate controls, as determined by counting the number of epithelial end buds (Fig. 1b, d). To determine if the size differences observed between wild type and *Galnt1*^{-/-} E12 SMGs were due to an overall developmental delay in the *Galnt1*^{-/-} animals, we also examined E12 kidneys, another branching organ that expresses *Galnt1* and develops at a similar time; however, *Galnt1* is not the most abundant *Galnt* family member in this tissue. There were no significant size differences between the developing E12 kidneys from *Galnt1*^{+/+}, *Galnt1*^{+/-} and *Galnt1*^{-/-} littermates (Supplementary Fig. S2), suggesting that the differences observed are specific to the SMGs (where *Galnt1* is the most abundant isoform) (Supplementary Fig. S1b). Examination of SMGs at later stages of development revealed that SMGs from *Galnt1*^{-/-} animals remain smaller into adulthood than *Galnt1*^{+/+} littermate controls (Supplementary Fig. S3).

Ex vivo SMG organ culture was employed to examine the growth of *Galnt1*-deficient SMGs by quantitating the number of end buds present after culture. Interestingly, E12 *Galnt1*^{-/-} SMGs grew significantly slower than wild type littermates in culture (Fig. 1b, e). Additionally, a less dramatic but significant reduction in growth was also seen for heterozygous *Galnt1*^{+/-} E12 SMGs grown in culture (Fig. 1b, e). Taken together, these results indicate that the loss of *Galnt1* leads to reduced initial epithelial bud size and reduced SMG growth at early stages of development.

Galnt1-deficient SMGs have an altered BM composition

It is known from previous studies that O-linked glycoproteins are typically abundant within the BM region of developing SMGs¹³. We therefore examined whether the epithelial BM was affected in *Galnt1*-deficient SMGs by staining for the major BM proteins (laminin and collagen IV) and total O-glycosylated proteins (as detected by the lectin peanut agglutinin, PNA) (Fig. 2). Significant decreases in both laminin and collagen IV were seen within the

BM of *Galnt1*^{-/-} SMGs when compared to wild type (Fig. 2a, c, d). Additionally, reductions in total O-glycosylated proteins present in the BM were also seen (Fig. 2a, b). No changes in E-cadherin staining around the periphery of epithelial cells were observed (Fig. 2), so we therefore used E-cadherin levels as an internal control to quantitate changes in the intensity of BM proteins. Reductions in laminin, collagen IV and PNA staining within the BM of *Galnt1*^{-/-} SMGs (expressed as a ratio with E-cadherin) were calculated and are shown in Fig. 2b, c, d. Interestingly, no changes in $\alpha 6$ integrin present along the basal region of the epithelial cells were observed between wild type and *Galnt1*^{-/-} SMGs (Supplementary Fig. S4), suggesting that the effects of *Galnt1* loss are specific to these secreted BM proteins. Additionally, no significant differences in laminin or collagen IV gene expression were detected among *Galnt1*^{+/+}, *Galnt1*^{+/-} and *Galnt1*^{-/-} SMGs (Fig. 2e), suggesting that the specific reduction in laminin and collagen in the BM is not due to a reduction in gene expression, but may be due to a defect in secretion.

Loss of *Galnt1* reduces BM secretion and induces ER stress

Further examination of E12 SMGs revealed an increase in intracellular staining for both laminin and collagen IV within the epithelial cells of *Galnt1*^{-/-} and *Galnt1*^{+/-} relative to wild type littermate controls (Fig. 2c, d). These results suggest that the loss of *Galnt1* affects secretion of BM components. To further explore this possibility, we examined secretory apparatus components within the SMG epithelial cells. Significant increases in the ER proteins Sec23 and calnexin were measured in the epithelial cells of *Galnt1*^{-/-} and *Galnt1*^{+/-} SMGs (Fig. 3a, b, c). Additionally, intracellular staining of laminin and collagen IV showed partial colocalization with the ER in cells of *Galnt1*^{-/-} and *Galnt1*^{+/-} SMGs (Fig. 3a), suggesting altered transport of these proteins through the secretory apparatus. As ER expansion and increases in calnexin are hallmarks of ER stress, we next examined whether ER stress and the unfolded protein response (UPR) were induced in *Galnt1*^{-/-} SMGs³⁸⁻⁴³. ER stress-dependent splicing of Xbp1 was seen in *Galnt1*^{-/-} and *Galnt1*^{+/-} SMGs, but not in *Galnt1*^{+/+} littermate controls (Fig. 3d). Additionally, ER stress-dependent translation of ATF4 and proteolytic cleavage of ATF6 were also observed in *Galnt1*^{-/-} SMGs, further indicating the induction of ER stress and the UPR (Fig. 3e). Furthermore, significant increases in the expression of the ER stress genes *Calnexin* (*Canx*) and *Edem1*, which are involved in protein folding, processing and degradation, were also observed in *Galnt1*-deficient SMGs relative to wild type (Fig. 3f). However, expression of *Chop*, an ER stress gene involved in the induction of apoptosis, was unaffected in *Galnt1*-deficient SMGs. Interestingly, these effects are distinct from those observed upon disruption of N-linked glycosylation by treatment with the inhibitor tunicamycin. Loss of N-glycosylation not only affected BM components and inhibited SMG growth, but also disrupted E-cadherin and $\alpha 6$ integrin localization; increased *Chop*, *Canx* and *Edem1* expression; and induced apoptosis (Supplementary Fig. S5a-f). Taken together, our results indicate that loss of *Galnt1* disrupts the specific secretion of BM proteins and induces certain aspects of the ER stress response.

Loss of *Galnt1* reduces FGF-mediated cell proliferation

To identify the mechanism by which loss of *Galnt1* affects SMG growth, we examined cell proliferation in E12 SMGs by EdU incorporation (Fig. 4). A significant reduction in epithelial cell proliferation in *Galnt1*^{-/-} SMGs was observed relative to heterozygotes and wild type SMGs (Fig. 4a, b). These results indicate that the decreased growth of *Galnt1*^{-/-} SMGs is due to a reduction in cell proliferation.

To determine the signaling pathways involved, we examined the expression of genes known to regulate SMG growth^{13,44}. qPCR revealed a specific decrease in the expression of *Fgf1* and a downstream target gene of Fgfr2b signaling, *Etv4*, in *Galnt1*^{-/-} SMGs relative to wild type and heterozygotes (Fig. 4c). Accordingly, in *Galnt1*-deficient glands, we measured a

specific decrease in phosphorylated AKT and MAPK (Fig. 4d), two kinases involved in FGF-mediated cell proliferation. Taken together, our data suggest that the loss of *Galnt1* affects BM secretion, which influences epithelial FGF-mediated signaling and cell proliferation during SMG development.

Exogenous laminin-111 rescues *Fgf1* expression and SMG growth

To demonstrate that the altered BM in *Galnt1*-deficient glands is responsible for the reduced growth and FGF signaling observed, we supplemented *Galnt1*-deficient glands with the major component of the embryonic BM (laminin-111) (Fig. 5 and Supplementary Fig. S6). The addition of laminin-111 to *Galnt1*-deficient SMGs restored *Fgf1* and *Etv4* expression as well as SMG growth (as assessed by both bud number and quantitation of total epithelial area) (Fig. 5a, b, c, d). In contrast, laminin-111 had no effect on SMG growth defects resulting from the loss of N-glycosylation (Supplementary Fig. S5a). It was previously shown that laminin mediates FGF signaling through $\beta 1$ integrin in the SMG¹². We therefore examined whether the laminin rescue of *Fgf1* and *Etv4* expression was dependent upon integrin function by using a $\beta 1$ integrin function-blocking antibody in the rescue experiments. As shown in Fig. 5d, the $\beta 1$ integrin function-blocking antibody abrogated laminin-111 rescue of *Fgf1* and *Etv4* expression and SMG growth. Taken together, our studies demonstrate that *Galnt1* influences SMG growth by modulating BM secretion, thereby affecting integrin signaling, AKT/MAPK phosphorylation and FGF signaling.

Discussion

Here, we demonstrate for the first time that loss of an O-glycosyltransferase causes pronounced effects on organogenesis and cell proliferation by altering the secretion of BM components. Our study provides mechanistic insight into how this conserved protein modification can impact developmental events by influencing the formation and composition of this highly specialized cellular microenvironment. The BM contains abundant matrix components, enzymes, proteases and growth factors that act in concert to ensure the proper growth and morphogenesis of the SMG during embryogenesis^{7,9,11–13,44}. Previous work has demonstrated that components of the BM as well as the enzymes that modify them are responsible for regulating SMG growth by influencing diverse signaling pathways^{7,9,11,12}. In particular, laminin is known to signal through $\beta 1$ integrins to specifically up-regulate *Fgf1*, *Fgfr1b* and *Fgfr2b*, thereby influencing FGF signaling^{12,44}. Here we show that the loss of an enzyme responsible for the initiation of O-glycosylation causes intracellular accumulation of laminin and collagen IV, concomitant with a reduction of each in the BM. Specific decreases in *Fgf1* expression, AKT and MAPK activation, and SMG growth were also seen in *Galnt1*^{-/-} SMGs. Interestingly, addition of exogenous laminin rescued FGF signaling and growth of *Galnt1*^{-/-} SMGs in a $\beta 1$ integrin-dependent manner. Therefore, we propose that the reduction of laminin in the BM of *Galnt1*-deficient SMGs results in decreased $\beta 1$ integrin signaling, with subsequent effects on *Fgf1* expression, FGF signaling and SMG growth (Fig. 6). This work provides the first example of the loss of an O-glycosyltransferase modulating cell signaling events by influencing the composition of the BM.

The specific mechanisms by which *Galnt1* affects the composition of the BM are currently under investigation. Previous work in *Drosophila* demonstrated that the catalytic activity of one family member was essential to mediate proper cell adhesion events by glycosylating a BM protein^{45,46}. Here, the glycosyltransferase encoded by *Galnt1* (ppGalNAcT-1) may also directly glycosylate BM proteins, influencing their folding, stability or trafficking through the secretory apparatus. Recent mass spectroscopy studies have demonstrated that many BM proteins, including dystroglycan, agrin and nidogen, are O-glycosylated in mammalian cells⁴⁷. And while laminin is known to be N-glycosylated, recent studies in both mammalian

and *Drosophila* cells have demonstrated that it is O-glycosylated as well^{47, 48}. Additionally, ppGalNAcT-1-mediated glycosylation of components of the secretory apparatus may also influence the proper trafficking and secretion of BM proteins as well as modulate the ER stress response. Recent work has demonstrated that Golgi and ER proteins known to be involved in secretion, secretory apparatus structure and ER stress are O-glycosylated, including calnexin, HSPA5, LMAN1 and MIA3⁴⁷. Therefore the direct targets of ppGalNAcT-1 that are responsible for mediating the biological effects observed may be numerous and diverse. However, the secretion changes observed in *Galnt1*^{-/-} SMGs affected BM proteins and not others, such as E-cadherin or $\alpha 6$ integrin. This is in contrast to the effects seen upon loss of N-glycosylation. Therefore, while N-glycosylation plays roles in global protein processing and transport, our results suggest a more specific role for *Galnt1* in the polarized secretion of certain BM components. Future studies will be focused on assessing which proteins are specifically glycosylated by ppGalNAcT-1 and how glycosylation influences their functions to mediate the developmental effects observed.

This study provides the first demonstration that the loss of a member of the *Galnt* family can induce ER stress. While the role of N-glycosylation in protein processing, transport and quality control is well-established^{22,23}, a role for O-linked glycosylation in these processes has not been described. However, recent studies have begun to elucidate a role for Golgi-resident enzymes in proteostasis and the ER stress response. siRNA-mediated knockdown of Golgi nucleotide sugar transporters (which provide sugar substrates for the glycosylation of macromolecules within the Golgi apparatus) decreased protein secretion and induced the ER stress response, illustrating a connection between the UPR and Golgi-based modifications⁴⁹. Additionally, a key player (ERManI) in the protein quality control system that targets proteins for ER-associated degradation (ERAD) has recently been identified as a Golgi-resident protein (and not an ER-resident protein, as previously thought), providing evidence for the role of the Golgi apparatus in sensing and tagging proteins destined to be degraded via ERAD⁵⁰. And finally, proteins involved in the ER stress response itself have recently been shown to be O-glycosylated, suggesting a role for this modification in their function⁴⁷. The data presented here demonstrate that the loss of *Galnt1* induces the ER stress response and the components responsible for increased protein folding and degradation, to reduce protein load in the secretory apparatus³⁸⁻⁴⁰. Interestingly, loss of *Galnt1* did not induce the apoptotic branch of the ER stress pathway, suggesting roles for O-glycosylation distinct from those of N-glycosylation. Altogether, these results highlight a dynamic interplay between the ER and the Golgi apparatus (and the enzymes which lie therein) in the regulation of protein processing, transport and quality control.

Our studies indicate a crucial role for *Galnt1* at early stages of SMG development, when *Galnt1* is the most abundantly expressed isoform. Interestingly, the reduction in growth and epithelial proliferation in *Galnt1*^{-/-} SMGs at early stages of development has a lasting impact on SMG size, as *Galnt1*^{-/-} SMGs remain significantly smaller than wild type at later stages of development and into adulthood (Supplementary Fig. S3). Whether reduced size affects the secretory capacity of the adult SMG is currently under investigation. Additionally, our results also provide evidence that *Galnt* heterozygosity may have biological consequences under certain circumstances. While *Galnt1*^{+/-} SMGs did not show overt growth defects when analyzed directly from the animal, they did display reduced growth when cultured ex vivo, suggesting that the loss of one copy of *Galnt1* can influence SMG growth under certain conditions. We hypothesize that *Galnt1* heterozygotes may represent a sensitized background, as evidenced by slight but significant changes in laminin and collagen levels present at the BM of *Galnt1*^{+/-} SMGs, as well as by changes related to an ER stress response. Thus, while these changes may not affect gland growth in vivo, they may influence SMG growth ex vivo under conditions that do not completely mimic the normal developmental environment. These results provide insight into how the loss of one

copy of a *Galnt* could contribute to disease susceptibility or predisposition by altering the cellular environment slightly, so as to make a cell or tissue more vulnerable/receptive to other genetic or environmental influences. Such a model may explain the heterozygosity of *GALNT12* seen in some colon cancer samples from a study demonstrating an association between the development of colon cancer and inactivating mutations in *GALNT12*³⁰.

In summary, this study reveals a novel role for one member of the conserved *Galnt* glycosyltransferase family in BM formation and FGF signaling during mammalian organogenesis. This work provides mechanistic insight into how O-glycosylation influences cell signaling and proliferation during development by regulating BM secretion and the ER stress response. As new genetic linkages are found between *Galnts* and various human diseases⁵¹, the role these enzymes play in the formation of the ECM and regulation of the proteostasis network needs to be considered.

Methods

Animal breeding

The *Galnt1* (previously designated ppGalNAcT-1)-deficient mice were the kind gift of Dr. Jamey Marth³⁷. *Galnt1*-deficient mice were backcrossed into the C57BL/6NHsd inbred mouse background for at least six generations before analysis³⁷. Heterozygous *Galnt1* animals (*Galnt1*^{+/-}) were crossed to generate embryos of the genotypes denoted (ASP protocol #08-498). Embryos were genotyped by PCR according to standard procedures³⁷. Wild type (*Galnt1*^{+/+}), heterozygous (*Galnt1*^{+/-}) and homozygous *Galnt1*-deficient (*Galnt1*^{-/-}) siblings were compared in all experiments.

Semi-quantitative RT-PCR

DNase-free RNA was prepared using an RNAqueous-Micro kit (Ambion, Inc.) and reverse-transcribed to make cDNA (Bio-Rad). Primers for *Galnt* and ER stress genes were designed using Beacon Designer software (Premier Biosoft) and are shown in Supplementary Tables S1 and S2. Other primers used were previously published and are available upon request^{11,12}. qPCR was performed for 40 cycles (95 °C for 10 seconds and 62 °C for 30 seconds) using SYBR-green PCR Master Mix, 1 ng of each cDNA sample and a My IQ real time PCR thermocycler or CFX96 Real-Time system (Bio-Rad). Gene expression was normalized to the housekeeping gene *29S*. Reactions were run in triplicate, and each experiment was repeated three times.

PCR to detect splicing of Xbp1 mRNA

Xbp1 PCR was performed using primers shown in Supplementary Table S2. Briefly, PCRs were performed for 35 cycles (94 °C for 30 seconds, 61 °C for 30 seconds and 72 °C for 90 seconds) in a Veriti™ thermal cycler (Applied Biosystems) using 10 ng of each cDNA sample. The PCR products were identified using a 4–12% acrylamide gel. Negative images of ethidium bromide-stained gels are shown.

Ex vivo SMG organ culture

SMGs from different stages were dissected and cultured on Nuclepore filters (VWR) as described¹³. Briefly, the filters were floated on 200 µl of DMEM-F12 in 50 mm glass-bottom microwell dishes (MatTek, MA). The culture medium contained 100 U ml⁻¹ penicillin, 100 µg ml⁻¹ streptomycin, 150 µg ml⁻¹ vitamin C and 50 µg ml⁻¹ transferrin. SMGs were cultured at 37 °C in a humidified 5% CO₂ incubator, and photographed at different time points. The epithelial buds were counted and E12 bud size was measured using ImageJ (NIH) software. Experiments were repeated at least three times.

Whole-mount immunofluorescence

SMGs were fixed with 4% PFA/PBS for 20 minutes at room temperature or with methanol/acetone (1:1) for 10 minutes at -20°C , and then blocked with 10% donkey serum, 1% BSA and M.O.M. blocking reagent (Vector Laboratories). Primary antibodies were diluted by M.O.M. protein reagent in PBS-0.1% Tween 20 and incubated at 4°C overnight. The following antibodies were used: Collagen IV (Ab769, Milipore; 1:200); E-cadherin (610182, BD Biosciences; 1:200); Laminin $\alpha 1$ (a gift from Dr. Takako Sasaki; 1:100)⁵²; Sec23 (E-19 sc-12107, Santa Cruz; 1:100); Calnexin (NB100-1965, Novus Biologicals; 1:100) and $\alpha 6$ integrin (GoH3, 555734, BD Biosciences; 1:100). After washing, SMGs were incubated with Cy3- and Cy5-conjugated secondary Fab fragment antibodies (Jackson Laboratories) and FITC-conjugated peanut agglutinin (PNA) (FL-1071, Vector Laboratories; 1:400). Stained SMGs were mounted and visualized on a Zeiss LSM 510 confocal microscope. Representative single section confocal images are shown in each figure. Images were analyzed by NIH ImageJ software and assembled in Photoshop.

Fluorescence signal quantification

Fluorescent intensity of confocal images was measured using NIH ImageJ software. Briefly, 6 single section confocal images separated by $0.5\ \mu\text{m}$ intervals were obtained for each SMG analyzed. Three regions within each single section were used to quantitate fluorescent signal intensity and these values were averaged to obtain a value for each marker for a particular SMG. The regions chosen for analysis centered on the BM (for PNA, laminin $\alpha 1$ and collagen IV) (each region was approximately $70\ \mu\text{m} \times 10\ \mu\text{m}$ in dimension), the epithelial region below the BM (for laminin $\alpha 1$ and collagen IV) (each region was approximately $70\ \mu\text{m} \times 40\ \mu\text{m}$) or the epithelial region including the BM (for E-cadherin, $\alpha 6$ integrin and EdU) (each region was approximately $70\ \mu\text{m} \times 50\ \mu\text{m}$). At least 3 SMGs of each genotype were analyzed.

Western blotting and analysis

Staged SMGs were lysed in RIPA buffer. Paired SMGs from *Galnt1*^{+/+}, *Galnt1*^{+/-} and *Galnt1*^{-/-} littermates were analyzed by SDS-PAGE under denaturing conditions and transferred to nitrocellulose membranes. For AKT/MAPK westerns, membranes were blocked with 5% BSA-TBST and probed with phospho- and total-AKT and MAPK (Erk1/2) antibodies (#9271, #9272, #4376, #9102, Cell Signaling Technology; 1:1000). To assess ER stress proteins by western, membranes were blocked with 2% BSA-PBST and probed with ATF4 (WH0000468M1, Sigma-Aldrich; 1:500), ATF6 (PRS3683, Sigma-Aldrich; 1:1000) or GAPDH (sc-25778, Santa Cruz; 1:2000). After washing, membranes were probed with HRP conjugated anti-mouse IgG (GE Healthcare; 1:5000) or HRP conjugated anti-rabbit IgG (Cell signaling Technology; 1:10,000). The HRP signal was detected using a chemiluminescent substrate (Thermo Scientific) and analyzed with a Fuji imager. NIH ImageJ was used to measure band intensity, and the ratios of ATF4/GAPDH or ATF6 (50 kDa)/GAPDH were determined for each genotype (setting the ratio for wild type littermate controls to 1).

Detection of cell proliferation

SMG epithelial proliferation was detected using the Click-iT 5-ethynyl-2'-deoxyuridine (EdU) imaging kit (C10337, Molecular Probes). $5\ \mu\text{M}$ EdU was added to SMG cultures and incubations proceeded for 30 min at 37°C . SMGs were then fixed in 4% PFA/PBS and permeabilized with 0.1% Triton X-100. Click-iT detection was performed using Alexa Fluor 488 azide. EdU detection is compatible with subsequent antibody and nuclear staining.

Laminin rescue experiments

E12 SMGs from each animal were separated and cultured, either with or without 80 $\mu\text{g ml}^{-1}$ exogenously added laminin-111 (3446-005-01, Trevigen, MD). Both treated and untreated SMGs were cultured for 2 days and then epithelial buds were counted and total epithelial area was measured using NIH ImageJ software; RNA was extracted from SMGs to perform qPCR. Preservative-free anti- $\beta 1$ integrin antibody (Ha2/5) and hamster control IgM (555002, 553957, BD Biosciences) were used for the $\beta 1$ integrin function-blocking experiments. 50 $\mu\text{g ml}^{-1}$ anti- $\beta 1$ integrin antibody or control IgM were added at the beginning of the culture period. 80 $\mu\text{g ml}^{-1}$ laminin-111 was added after 30 minutes to both control IgM and $\beta 1$ integrin antibody treated SMGs. Cultures were continued for 2 days, after which SMGs were collected for analysis and RNA extraction. Experiments were repeated four times.

Statistical analyses

Values were plotted as means \pm standard errors of the mean for each group from three or more experiments. Student's *t*-test was used to calculate *P*-values.

Supplementary Material

Refer to Web version on PubMed Central for supplementary material.

Acknowledgments

We would like to sincerely thank our colleagues for many helpful discussions. We thank Drs. Vaishali Patel and Ivan Rebutini for their assistance, and Drs. Lawrence Tabak, Jamey Marth and Yu Guan for providing *Galnt1*-deficient mice. We also thank Shelagh Johnson for editorial assistance. This research was supported by the Intramural Research Program of the NIDCR at the National Institutes of Health.

References

1. Bissell MJ, Radisky D. Putting tumours in context. *Nat. Rev. Cancer.* 2001; 1:46–54. [PubMed: 11900251]
2. Pupa SM, Menard S, Forti S, Tagliabue E. New insights into the role of extracellular matrix during tumor onset and progression. *J. Cell Physiol.* 2002; 192:259–267. [PubMed: 12124771]
3. Mueller MM, Fusenig NE. Friends or foes - bipolar effects of the tumour stroma in cancer. *Nat. Rev. Cancer.* 2004; 4:839–849. [PubMed: 15516957]
4. Weigelt B, Bissell MJ. Unraveling the microenvironmental influences on the normal mammary gland and breast cancer. *Semin. Cancer Biol.* 2008; 18:311–321. [PubMed: 18455428]
5. Poschl E, et al. Collagen IV is essential for basement membrane stability but dispensable for initiation of its assembly during early development. *Development.* 2004; 131:1619–1628. [PubMed: 14998921]
6. Sasaki T, Fassler R, Hohenester E. Laminin: the crux of basement membrane assembly. *J. Cell Biol.* 2004; 164:959–963. [PubMed: 15037599]
7. Sakai T, Larsen M, Yamada KM. Fibronectin requirement in branching morphogenesis. *Nature.* 2003; 423:876–881. [PubMed: 12815434]
8. Kadoya Y, Yamashina S. Salivary gland morphogenesis and basement membranes. *Anat. Sci. Int.* 2005; 80:71–79. [PubMed: 15960312]
9. Patel VN, Rebutini IT, Hoffman MP. Salivary gland branching morphogenesis. *Differentiation.* 2006; 74:349–364. [PubMed: 16916374]
10. Patel VN, et al. Heparanase cleavage of perlecan heparan sulfate modulates FGF10 activity during ex vivo submandibular gland branching morphogenesis. *Development.* 2007; 134:4177–4186. [PubMed: 17959718]

11. Rebutini IT, et al. MT2-MMP-dependent release of collagen IV NC1 domains regulates submandibular gland branching morphogenesis. *Dev. Cell.* 2009; 17:482–493. [PubMed: 19853562]
12. Rebutini IT, et al. Laminin alpha5 is necessary for submandibular gland epithelial morphogenesis and influences FGFR expression through beta1 integrin signaling. *Dev. Biol.* 2007; 308:15–29. [PubMed: 17601529]
13. Hoffman MP, et al. Gene expression profiles of mouse submandibular gland development: FGFR1 regulates branching morphogenesis in vitro through BMP- and FGF-dependent mechanisms. *Development.* 2002; 129:5767–5778. [PubMed: 12421715]
14. Patel VN, et al. Specific heparan sulfate structures modulate FGF10-mediated submandibular gland epithelial morphogenesis and differentiation. *J. Biol. Chem.* 2008; 283:9308–9317. [PubMed: 18230614]
15. Hart GW, Copeland RJ. Glycomics hits the big time. *Cell.* 2010; 143:672–676. [PubMed: 21111227]
16. Tabak LA. The role of mucin-type O-glycans in eukaryotic development. *Semin. Cell Dev. Biol.* 2010; 21:616–621. [PubMed: 20144722]
17. Schachter H. Mgat1-dependent N-glycans are essential for the normal development of both vertebrate and invertebrate metazoans. *Semin. Cell Dev. Biol.* 2010; 21:609–615. [PubMed: 20206280]
18. Liu L, Xu YX, Hirschberg CB. The role of nucleotide sugar transporters in development of eukaryotes. *Semin Cell Dev. Biol.* 2010; 21:600–608. [PubMed: 20144721]
19. Nakamura N, Lyalin D, Panin VM. Protein O-mannosylation in animal development and physiology: from human disorders to *Drosophila* phenotypes. *Semin. Cell Dev. Biol.* 2010; 21:622–630. [PubMed: 20362685]
20. Takeuchi H, Haltiwanger RS. Role of glycosylation of Notch in development. *Semin. Cell Dev. Biol.* 2010; 21:638–645. [PubMed: 20226260]
21. Love DC, Krause MW, Hanover JA. O-GlcNAc cycling: emerging roles in development and epigenetics. *Semin. Cell Dev. Biol.* 2010; 21:646–654. [PubMed: 20488252]
22. Roth J, et al. Protein N-glycosylation, protein folding, and protein quality control. *Mol. Cells.* 2010; 30:497–506. [PubMed: 21340671]
23. Maattanen P, Gehring K, Bergeron JJ, Thomas DY. Protein quality control in the ER: the recognition of misfolded proteins. *Semin. Cell Dev. Biol.* 2010; 21:500–511. [PubMed: 20347046]
24. Tian E, Ten Hagen KG. Recent insights into the biological roles of mucin-type O-glycosylation. *Glycoconj. J.* 2009; 26:325–334. [PubMed: 18695988]
25. Ten Hagen KG, Tran DT. A UDP-GalNAc:polypeptide N-acetylgalactosaminyltransferase is essential for viability in *Drosophila melanogaster*. *J. Biol. Chem.* 2002; 277:22616–22622. [PubMed: 11925446]
26. Schwientek T, et al. Functional conservation of subfamilies of putative UDP-N-acetylgalactosamine: polypeptide N-acetylgalactosaminyltransferases in *Drosophila*, *Caenorhabditis elegans*, and mammals. One subfamily composed of I(2)35Aa is essential in *Drosophila*. *J. Biol. Chem.* 2002; 277:22623–22638. [PubMed: 11925450]
27. Tian E, Ten Hagen KG. A UDP-GalNAc:polypeptide N-acetylgalactosaminyltransferase is required for epithelial tube formation. *J. Biol. Chem.* 2007; 282:606–614. [PubMed: 17098739]
28. Tran D, et al. Multiple members of the UDP-GalNAc:polypeptide N-acetylgalactosaminyltransferase family are essential for viability in *Drosophila*. *J. Biol. Chem.* 2012; 287:5243–5252. [PubMed: 22157008]
29. Fuster MM, Esko JD. The sweet and sour of cancer: glycans as novel therapeutic targets. *Nat. Rev. Cancer.* 2005; 5:526–542. [PubMed: 16069816]
30. Guda K, et al. Inactivating germ-line and somatic mutations in polypeptide N-acetylgalactosaminyltransferase in human colon cancers. *Proc. Natl. Acad. Sci. U S A.* 2009; 106:12921–12925. [PubMed: 19617566]
31. Topaz O, et al. Mutations in GALNT3, encoding a protein involved in O-linked glycosylation, cause familial tumoral calcinosis. *Nat. Genet.* 2004; 36:579–581. [PubMed: 15133511]

32. Ichikawa S, Lyles KW, Econs MJ. A novel GALNT3 mutation in a pseudoautosomal dominant form of tumoral calcinosis: evidence that the disorder is autosomal recessive. *J. Clin. Endocrinol. Metab.* 2005; 90:2420–2423. [PubMed: 15687324]
33. Ju T, Cummings RD. Protein glycosylation: chaperone mutation in Tn syndrome. *Nature.* 2005; 437:1252. [PubMed: 16251947]
34. Kathiresan S, et al. Six new loci associated with blood low-density lipoprotein cholesterol, high-density lipoprotein cholesterol or triglycerides in humans. *Nat. Genet.* 2008; 40:189–197. [PubMed: 18193044]
35. Willer CJ, et al. Newly identified loci that influence lipid concentrations and risk of coronary artery disease. *Nat. Genet.* 2008; 40:161–169. [PubMed: 18193043]
36. Teslovich TM, et al. Biological, clinical and population relevance of 95 loci for blood lipids. *Nature.* 2010; 466:707–713. [PubMed: 20686565]
37. Tenno M, et al. Initiation of protein O glycosylation by the polypeptide GalNAcT-1 in vascular biology and humoral immunity. *Mol. Cell. Biol.* 2007; 27:8783–8796. [PubMed: 17923703]
38. Mori K. Signalling pathways in the unfolded protein response: development from yeast to mammals. *J. Biochem.* 2009; 146:743–750. [PubMed: 19861400]
39. Kapoor A, Sanyal AJ. Endoplasmic reticulum stress and the unfolded protein response. *Clin. Liver Dis.* 2009; 13:581–590. [PubMed: 19818306]
40. Hetz C. The unfolded protein response: controlling cell fate decisions under ER stress and beyond. *Nature Rev.* 2012; 13:89–102.
41. Calton M, et al. IRE-1 couples endoplasmic reticulum load to secretory capacity by processing the XBP-1 mRNA. *Nature.* 2002; 415:92–96. [PubMed: 11780124]
42. Haze K, et al. Mammalian transcription factor ATF6 is synthesized as a transmembrane protein and activated by proteolysis in response to endoplasmic reticulum stress. *Molec. Biol. Cell.* 1999; 10:3787–3799. [PubMed: 10564271]
43. Fatma N, et al. Deficiency of Prdx6 in lens epithelial cells induces ER stress response-mediated impaired homeostasis and apoptosis. *Am. J. Physiol. Cell Physiol.* 2011; 301:C954–C967. [PubMed: 21677259]
44. Steinberg Z, et al. FGFR2b signaling regulates ex vivo submandibular gland epithelial cell proliferation and branching morphogenesis. *Development.* 2005; 132:1223–1234. [PubMed: 15716343]
45. Zhang L, Tran DT, Ten Hagen KG. An O-glycosyltransferase promotes cell adhesion during development by influencing secretion of an extracellular matrix integrin ligand. *J. Biol. Chem.* 2010; 285:19491–19501. [PubMed: 20371600]
46. Zhang L, Zhang Y, Ten Hagen KG. A mucin-type O-glycosyltransferase modulates cell adhesion during *Drosophila* development. *J. Biol. Chem.* 2008; 283:34076–34086. [PubMed: 18835818]
47. Steentoft C, et al. Mining the O-glycoproteome using zinc-finger nuclease-glycoengineered SimpleCell lines. *Nat. Methods.* 2011; 8:977–982. [PubMed: 21983924]
48. Schwientek T, et al. A serial lectin approach to the mucin-type O-glycoproteome of *Drosophila melanogaster* S2 cells. *Proteomics.* 2007; 7:3264–3277. [PubMed: 17708590]
49. Xu YX, Liu L, Caffaro CE, Hirschberg CB. Inhibition of Golgi apparatus glycosylation causes endoplasmic reticulum stress and decreased protein synthesis. *J. Biol. Chem.* 2010; 285:24600–24608. [PubMed: 20529871]
50. Pan S, et al. Golgi localization of ERManI defines spatial separation of the mammalian glycoprotein quality control system. *Mol. Biol. Cell.* 2011; 22:2810–2822. [PubMed: 21697506]
51. Fakhro KA, et al. Rare copy number variations in congenital heart disease patients identify unique genes in left-right patterning. *Proc. Natl. Acad. Sci. U S A.* 2011; 108:2915–2920. [PubMed: 21282601]
52. Sasaki T, Giltay R, Talts U, Timpl R, Talts JF. Expression and distribution of laminin alpha1 and alpha2 chains in embryonic and adult mouse tissues: an immunochemical approach. *Exp. Cell Res.* 2002; 275:185–199. [PubMed: 11969289]
53. Bassett KE, Spooner BS. An autoradiographic analysis of N-linked glycoconjugates in embryonic salivary gland morphogenesis. *J. Exp. Zool.* 1987; 242:317–324. [PubMed: 2956359]

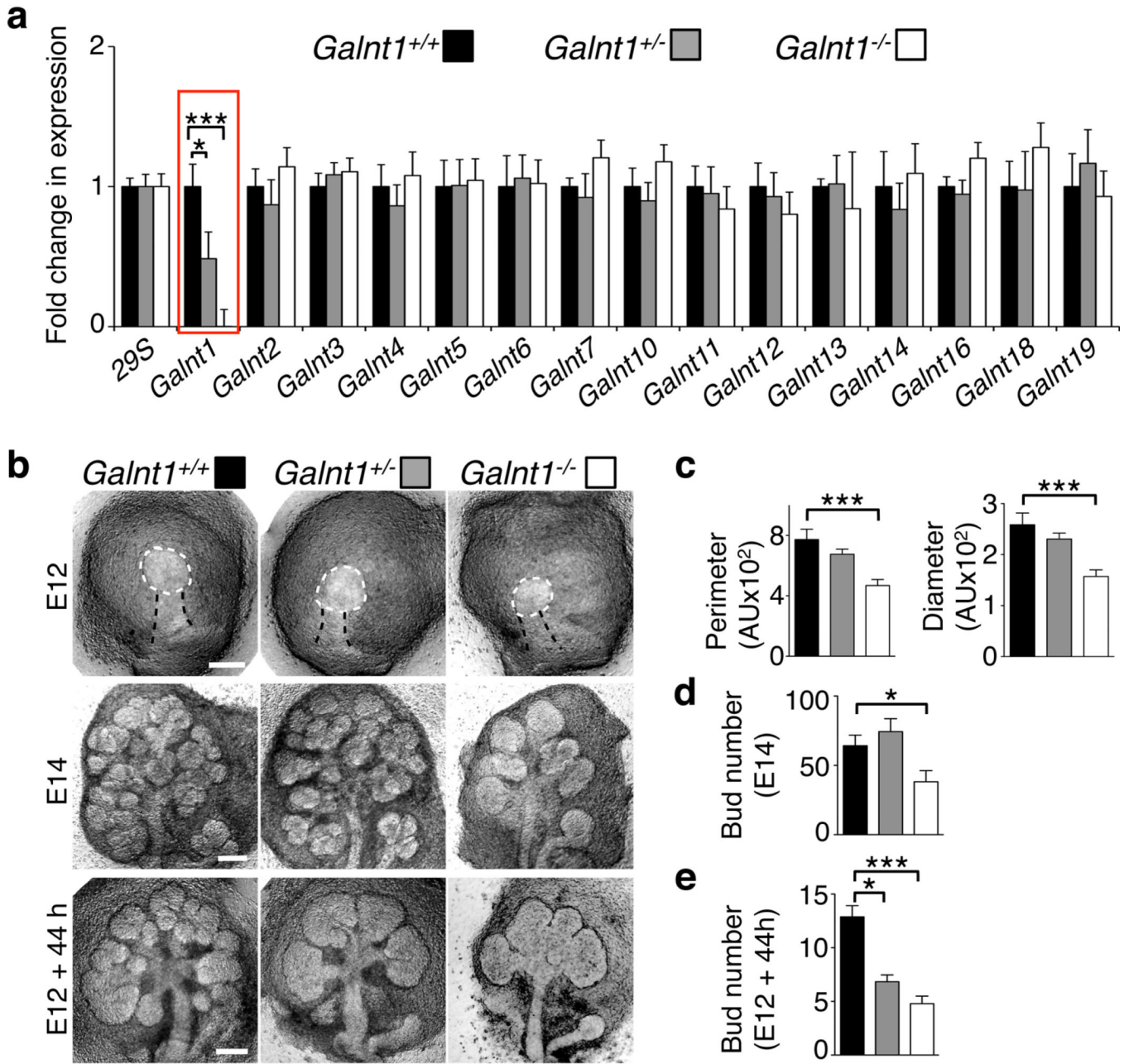


Figure 1. Loss of *Galnt1* results in smaller epithelial buds and reduced SMG growth

(a) Loss of *Galnt1* expression (highlighted in red box) in SMGs from *Galnt1*-deficient mice was verified by qPCR. Expression of other *Galnt* family members is unchanged in *Galnt1*-deficient SMGs. Expression was normalized to *29S*. (b) Loss of *Galnt1* results in smaller E12 epithelial buds and reduced SMG growth. E12 SMGs from wild type (*Galnt1*^{+/+}; n=31), *Galnt1* heterozygotes (*Galnt1*^{+/-}; n=74) and *Galnt1*-deficient (*Galnt1*^{-/-}; n=36) embryos were isolated and epithelial bud size (white dashed line) was measured. E14 SMGs from *Galnt1*^{+/+} (n=26), *Galnt1*^{+/-} (n=38) and *Galnt1*^{-/-} (n=16) were isolated and bud number was counted. E12 SMGs from *Galnt1*^{+/+} (n=9), *Galnt1*^{+/-} (n=21) and *Galnt1*^{-/-} (n=10) were grown for 44 hrs in ex vivo culture and total bud number was counted. (c) Average perimeter and diameter of E12 epithelial buds from each genotype. (d) Average

bud number present in E14 SMGs from each genotype. (e) Average bud number present after culturing each genotype for 44 hrs. Student's *t*-test was used to calculate P-values. *, $P < 0.05$; ***, $P < 0.001$.

\$watermark-text

\$watermark-text

\$watermark-text

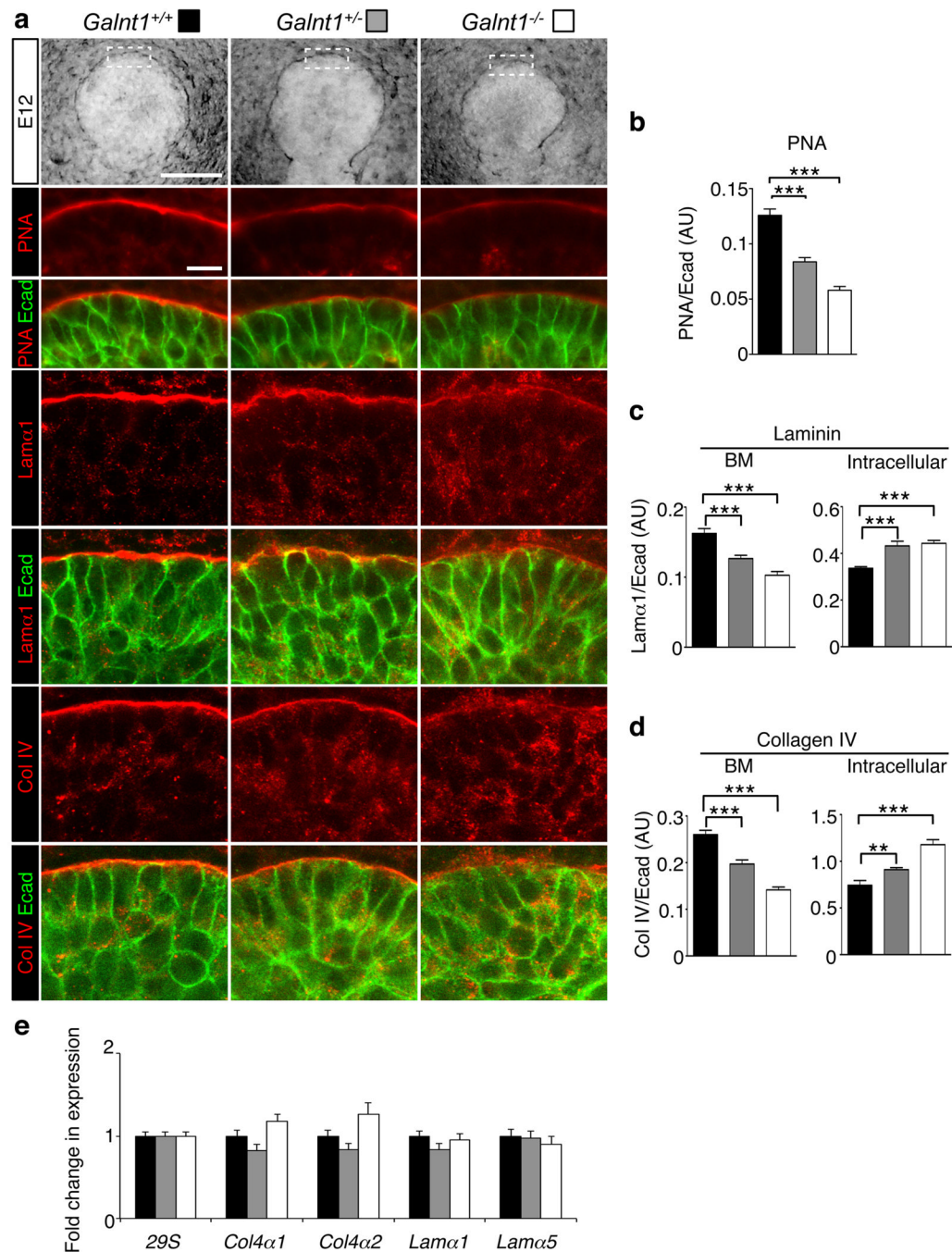


Figure 2. Loss of *Galnt1* causes reduction in ECM proteins and O-glycans in the BM of E12 SMGs

(a) Phase contrast images of E12 SMGs (top row) highlight the region (white dashed box) of high magnification views in the single section confocal images shown below.

Immunofluorescence analysis of wild type (*Galnt1*^{+/+}), *Galnt1* heterozygotes (*Galnt1*^{+/-}) and *Galnt1*-deficient (*Galnt1*^{-/-}) E12 SMGs revealed a specific decrease in laminin α 1 (Lam α 1, red), collagen IV (Col IV, red) and O-glycans (detected by the peanut agglutinin lectin, PNA, red) in the BM of *Galnt1*^{-/-} SMGs. Additionally, intracellular accumulation of laminin α 1 and collagen IV in epithelial cells was observed. No changes in E-cadherin (Ecad, green) were seen in *Galnt1*^{-/-} SMGs. (b) PNA staining intensity along the BM region

for each genotype (expressed as a ratio relative to total levels of E-cadherin) was graphed. Staining intensities of $\text{Lam}\alpha 1$ (**c**) and Col IV (**d**) along the BM and within the epithelial cells were graphed. 5 SMGs of each genotype from four independent crosses were examined. (**e**) Expression of major BM genes is unchanged in *Galnt1*-deficient SMGs. Expression was normalized to *29S*. Scale bar=100 μm for phase contrast images and 10 μm for confocal images. Student's *t*-test was used to calculate *P*-values. **, $P < 0.01$, ***, $P < 0.001$.

\$watermark-text

\$watermark-text

\$watermark-text

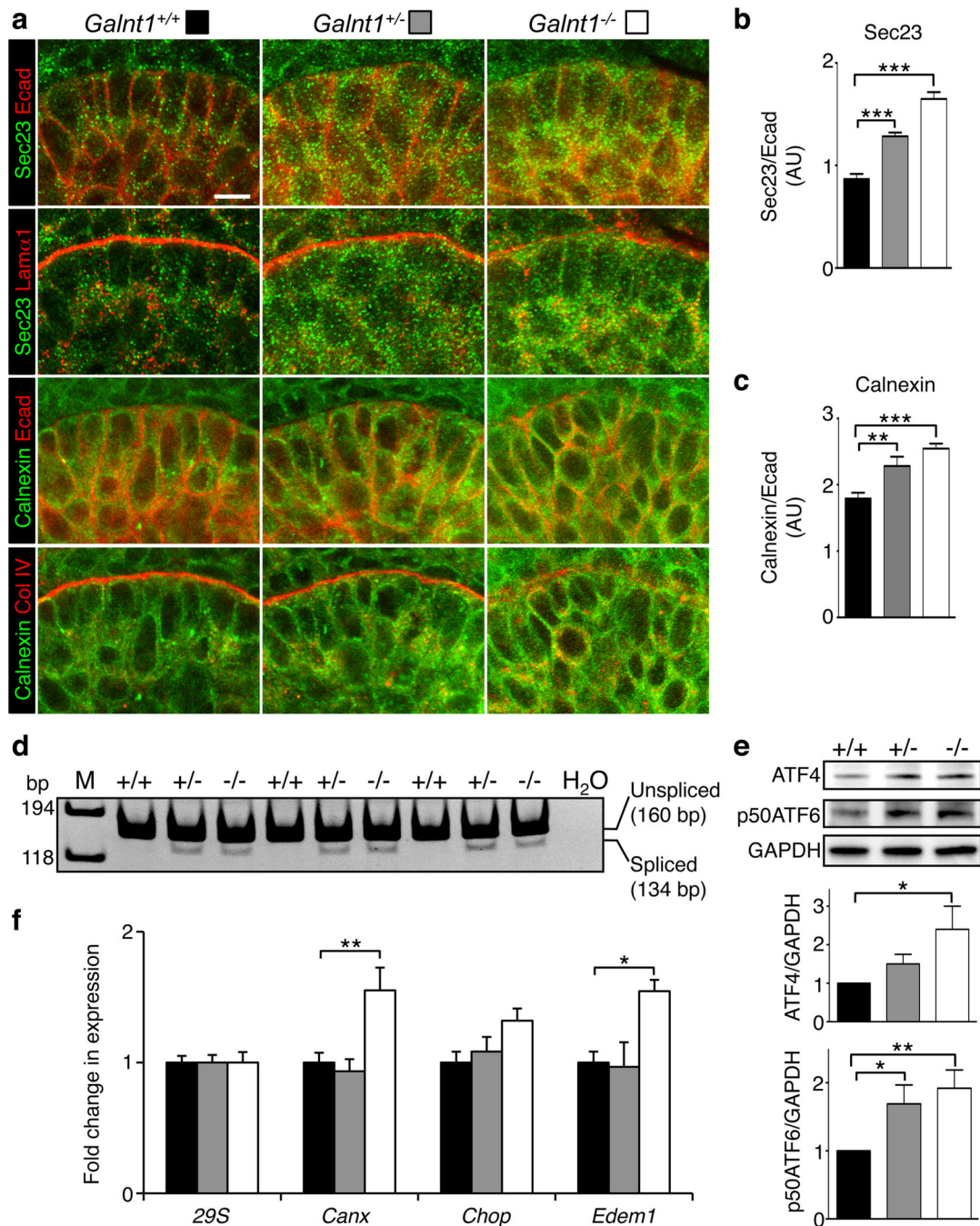


Figure 3. Loss of *Galnt1* affects secretion of BM proteins and induces ER stress in E12 SMGs
(a) Immunofluorescence analysis of *Galnt1*^{+/+}, *Galnt1*^{+/-} and *Galnt1*^{-/-} E12 SMGs. SMGs were stained for the ER marker Sec23 (green) and laminin α 1 (Lam α 1, red) or the ER marker calnexin (green) and collagen IV (Col IV, red) revealed partial colocalization of these BM proteins with the ER in *Galnt1*^{-/-} SMGs. SMGs were also costained with E-cadherin (Ecad, red). Graphs of the ratios of Sec23/Ecad (**b**) and calnexin/Ecad (**c**) show an increase in staining for these ER markers in *Galnt1*^{-/-} epithelial cells. **(d)** ER stress-dependent splicing of Xbp1 is detected in *Galnt1*^{+/-} and *Galnt1*^{-/-} E12 SMGs by PCR. Reaction products in each lane are from cDNA prepared from a pair of E12 SMGs of the

genotype denoted above each lane. M=size markers. H₂O=control reaction without cDNA added. Negative images of ethidium bromidestained gels are shown. **(e)** ER stress-dependent increases in ATF4 protein and the 50kDa cleaved form of ATF6 (p50ATF6) were seen in *Galnt1*^{-/-} E12 SMGs relative to *Galnt1*^{+/+} and *Galnt1*^{+/-} littermate controls. Levels of ATF4 and p50ATF6 were normalized to GAPDH and ratios were graphed. Ratios of AFT4/GAPDH and p50ATF6/GAPDH in *Galnt1*^{+/+} SMGs were set to 1. Graphs represent the average of 5 independent experiments for each genotype. **(f)** Increases in the expression of specific ER stress genes in *Galnt1*^{-/-} E12 SMGs relative to *Galnt1*^{+/+} and *Galnt1*^{+/-} littermate controls. Gene expression levels (from 5 SMGs of each genotype from three crosses) were determined by qPCR. Expression was normalized to *29S*. Scale bar=10μm. Student's *t*-test was used to calculate *P*-values. *, *P*<0.05; **, *P*<0.01; ***, *P*<0.001

\$watermark-text

\$watermark-text

\$watermark-text

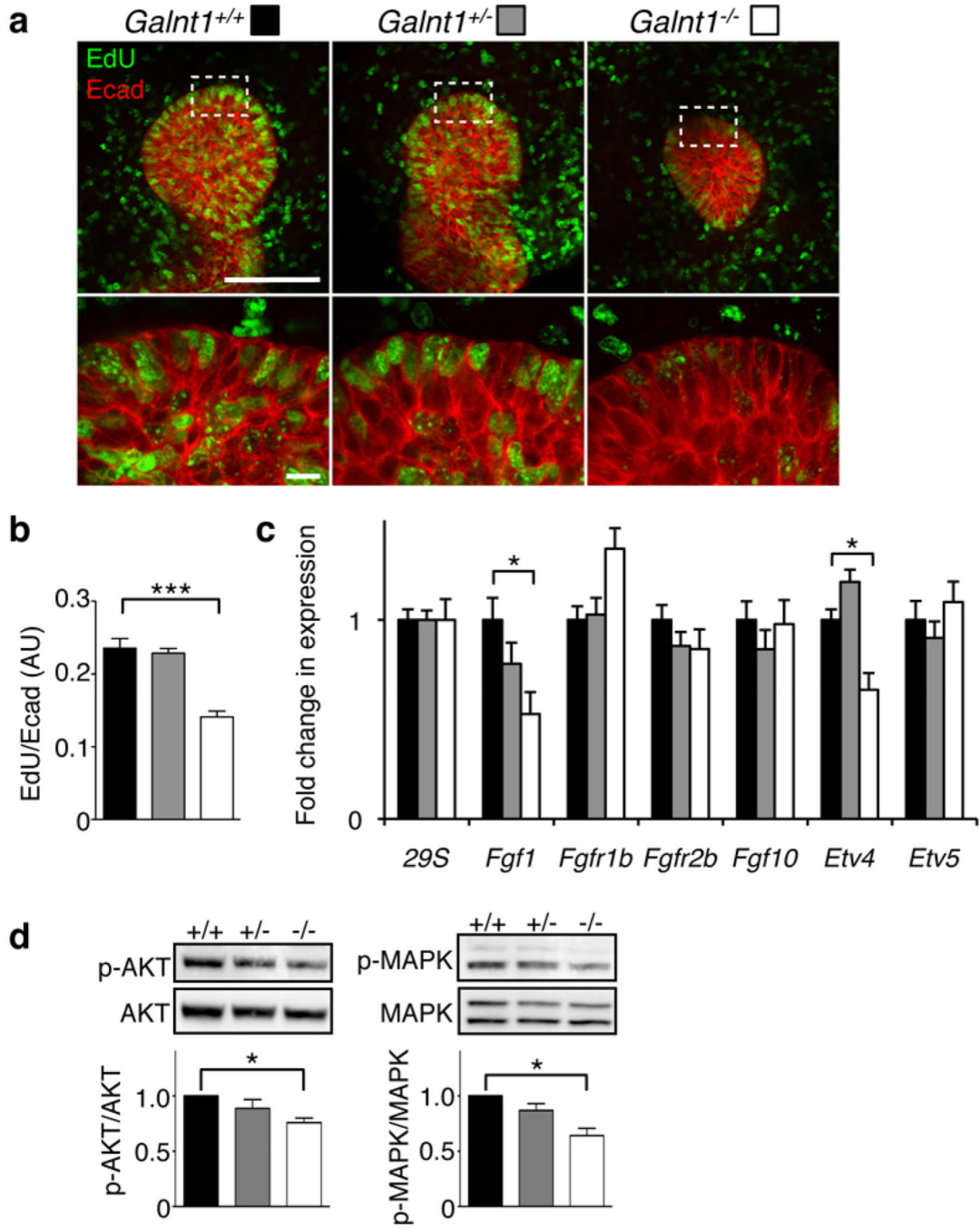


Figure 4. Loss of *Galnt1* causes reduced cell proliferation and FGF signaling
(a) EdU labeling (green) of *Galnt1*^{+/+}, *Galnt1*^{+/-} and *Galnt1*^{-/-} E12 SMGs showed decreased epithelial cell proliferation in *Galnt1*^{-/-} SMGs. Glands were also co-stained with E-cadherin (Ecad, red). The white dash boxes in low magnification images indicate the location of the high magnification views below. Scale bars = 100 μm for low magnification and 10 μm for high magnification. **(b)** Average ratios of EdU/E-cadherin for each genotype are shown. 4 SMGs of each genotype from three independent crosses were examined. **(c)** *Fgf1* and *Etv4* expression were specifically decreased in *Galnt1*^{-/-} E12 SMGs as determined by qPCR. Expression was normalized to *29S*. **(d)** Decreased AKT and MAPK

phosphorylation was seen in *Galnt1*^{-/-} E12 SMGs relative to *Galnt1*^{+/+} and *Galnt1*^{+/-} littermate controls. Graphs are the average of values obtained from 5 SMGs of each genotype. Student's *t*-test was used to calculate *P*-values. *, *P*<0.05; ***, *P*<0.001.

\$watermark-text

\$watermark-text

\$watermark-text

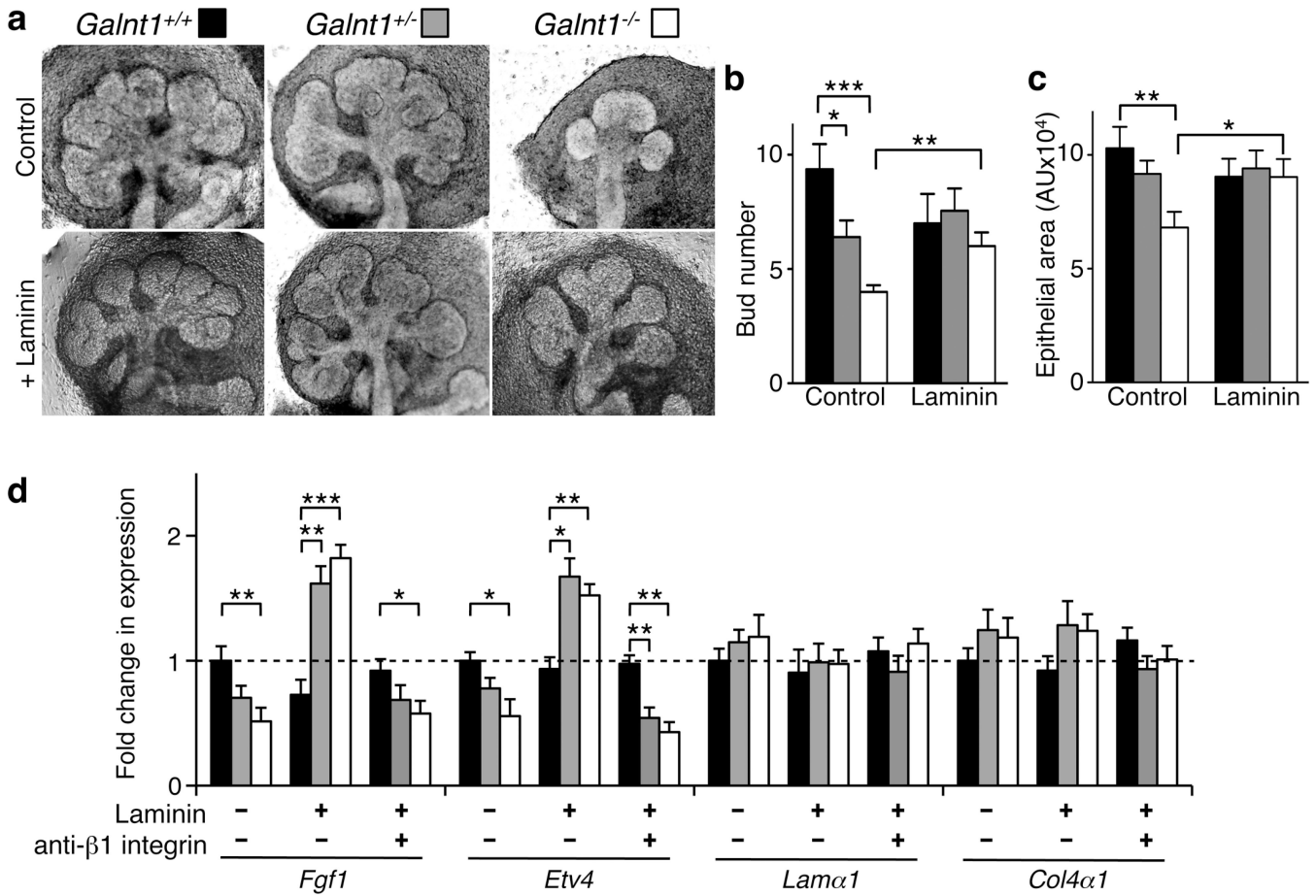


Figure 5. Exogenous BM components rescue *Galnt1*^{-/-} growth defects as well as *Fgf1* and *Etv4* expression in a β1 integrin-dependent manner

(a) *Galnt1*^{+/+} (n=11), *Galnt1*^{+/-} (n=20) and *Galnt1*^{-/-} (n=9) E12 SMGs were untreated (Control) or treated with 80 μg ml⁻¹ laminin-111 (+ Laminin) for 48 hrs. The average bud number (b) and epithelial area (c) present after culturing E12 SMGs for 48 hrs in the presence or absence of laminin revealed that growth was restored in *Galnt1*^{-/-} SMGs. (d) Laminin addition to *Galnt1*-deficient SMGs rescued *Fgf1* and *Etv4* expression, as determined by qPCR. However, laminin rescue of *Fgf1* and *Etv4* expression in *Galnt1*^{-/-} SMGs is abrogated in the presence of β1 integrin function blocking antibody, as determined by qPCR. Student's *t*-test was used to calculate *P*-values. *, *P*<0.05; **, *P*<0.01; ***, *P*<0.001.

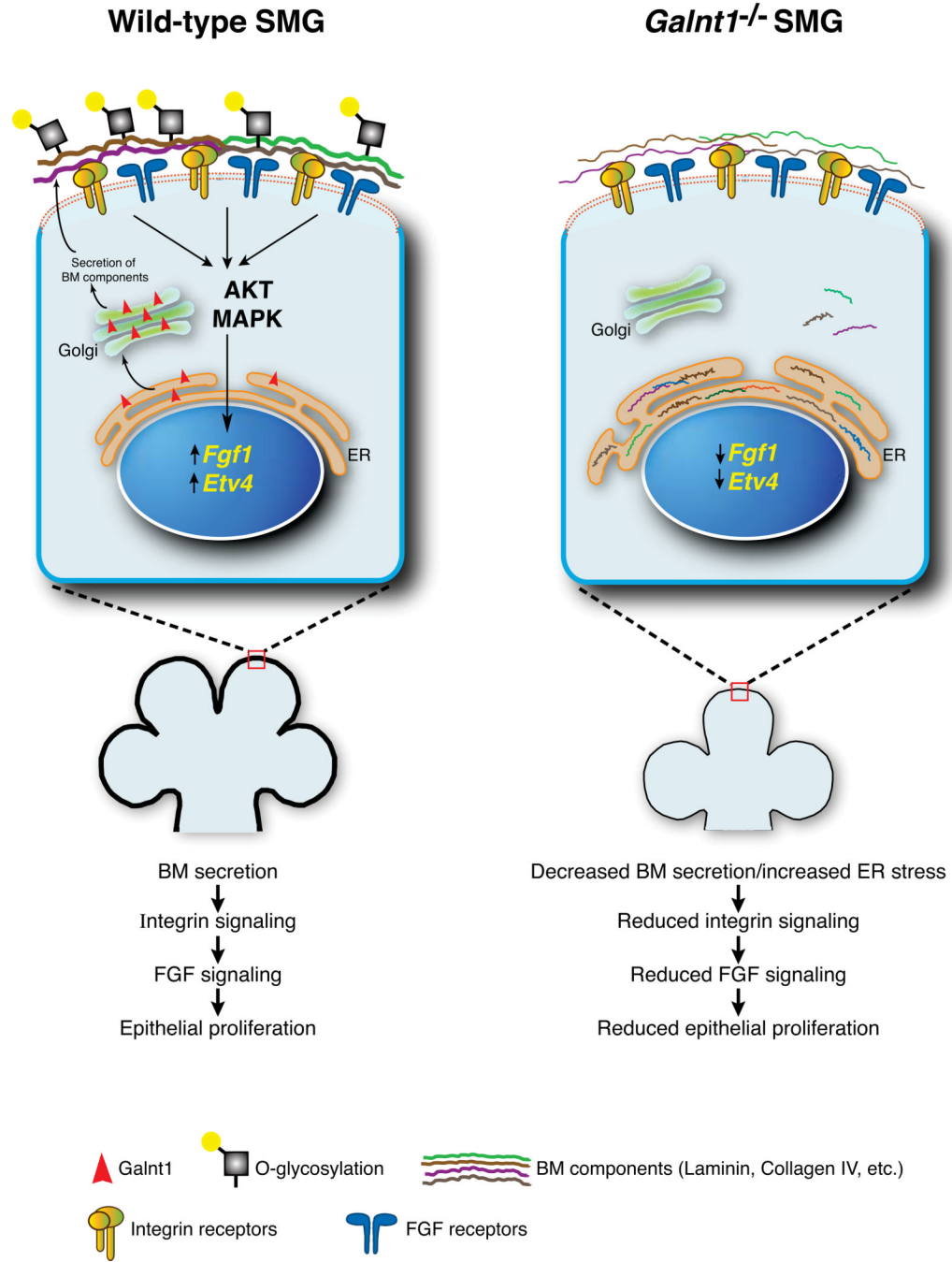


Figure 6. Working model showing how *Galnt1* influences BM composition and *Fgf1*-mediated SMG proliferation

Loss of *Galnt1* results in reduced secretion of BM components, causing induction of the ER stress response. Altered BM composition in *Galnt1*^{-/-} SMGs causes reduced signaling by laminin through $\beta 1$ integrin receptors, resulting in decreased *Fgf1* and *Etv4* expression, reduced AKT/MAPK phosphorylation and reduced epithelial cell proliferation.